Journal of The Electrochemical Society, **147** (4) 1332-1337 (2000)
S0013-4651(99)09-056-4 CCC: $7.00 © The Electrochemical Society, Inc.

Intermediate Temperature Solid Oxide Fuel Cells Using $LaGaO_3$ Electrolyte

II. Improvement of Oxide Ion Conductivity and Power Density by Doping Fe for Ga Site of $LaGaO_3$

Tatsumi Ishihara,*,z Takaaki Shibayama, Miho Honda, Hiroyasu Nishiguchi, and Yusaku Takita

Department of Applied Chemistry, Faculty of Engineering, Oita University, Oita 870-1192 , Japan

Effects of small amounts of Fe doping for Ga site in $LaGaO_3$-based oxide on oxide ion conductivity is investigated in this study. It is found that doping a small amount of Fe is effective for improving the oxide ion conductivity in $La_{0.8}Sr_{0.2}Ga_{0.8}Mg_{0.2}O_3$ (LSGM). The highest oxide ion conductivity was exhibited at $x = 0.03$ in $La_{0.8}Sr_{0.2}Ga_{0.8}Mg_{0.2-x}Fe_xO_3$ among the Fe-doped samples. Electron spin resonance (ESR) measurements suggest that Fe is trivalent in $LaGaO_3$ lattice. The application of the Fe-doped $LaGaO_3$-based oxide for the electrolyte of solid oxide fuel cell was further investigated. Power density of the solid oxide fuel cell was increased by using Fe-doped LSGM for electrolyte. This can be explained by the decrease in electrical resistance loss by improving the oxide ion conductivity. A maximum power density close to 700 mW/cm^2 was obtained at 1073 K on the cell using 0.5 mm thick $La_{0.8}Sr_{0.2}Ga_{0.8}Mg_{0.17}Fe_{0.03}O_3$ (LSGMF) and O_2 as the electrolyte and the oxidant, respectively. Therefore, close to the theoretical open-circuit potential was exhibited by the LSGMF cell. On the other hand, the power density was slightly smaller than that of the cell using Co-doped LSGM as electrolyte, especially, at temperatures lower than 973 K. This may result from the large activation energy for ion conductivity. However, the power density of the LSGMF cell was higher than that of the LSGM cell. Therefore, LSGM doped with a small amount of Fe is a promising electrolyte similar to Co-doped LSGM for the intermediate solid oxide fuel cell.

Manuscript submitted September 14, 1999; revised manuscript received December 21, 1999.

Solid oxide fuel cells (SOFC) provide a new and clean electric power generating system At present, Y_2O_3-stabilized ZrO_2 (YSZ) is commonly used as the electrolyte of a solid oxide fuel cell. Since the oxide ion conductivity of YSZ is insufficient for the electrolyte of fuel cells, a thin electrolyte film without gas leakage and an excessively high operating temperature such as 1273 K are essential for the high power density of SOFCs when YSZ is used as electrolyte. On the other hand, all the advantages of SOFC such as a high efficiency and a variety of usable fuels can be obtained at decreased temperatures such as 1073 K. Furthermore, the choice of the materials for cell construction becomes wider; in particular, cheap refractory metals such as a stainless steel will be usable by decreasing the operating temperature to 900 K. Consequently, decrease in operating temperature is an important subject for the development of the cheap but the reliable SOFCs.[1] In order to develop the intermediate temperature SOFC, an active electrode, in particular, the cathode electrode catalyst, and an electrolyte with a low resistance are essential. Ceria doped with Gd or Sm is considered for the candidate electrolyte of the intermediate temperature SOFC.[2] However, ceria-based oxide exhibits a significant electronic conduction in the reducing atmosphere,[2] which causes various problems for the application of SOFC.[3-5] On the other hand, preparation of a very thin YSZ film (less than 10 μm thick) is another solution method for decreasing the operating temperature, and various methods are now under investigation.[6]

Except for making a very thin YSZ film, it is of great importance for the intermediate temperature SOFCs to develop new electrolyte materials which exhibit a high oxide ion conduction over a wide range of oxygen partial pressures. In our previous study, the oxide ion conductivity in the perovskite oxide was investigated, and it was found that the $LaGaO_3$-based perovskite-type oxide exhibits high oxide ion conductivity,[7,8] which is comparable to that of CeO_2-based oxide. In particular, $LaGaO_3$ doped with Sr for La and Mg for Ga sites (denoted as LSGM) exhibits a high oxide ion conductivity stably over a wide range of oxygen partial pressure.[9-12] It is generally believed that doping with a transition metal cation is undesirable for the ionic conductor due to the appearance of electron or hole conduction.[13] However, it was found that the oxide ion conductivity was also improved by doping Co for Ga site of LSGM, although hole conduction appeared slightly in the high oxygen partial pressure range. Furthermore, it became clear that the application of Co-doped LSGM for the electrolyte of SOFC greatly improves the power density of the cells at low temperature. On the other hand, it was found that doping Fe also has similar positive effects on the electrical conductivity in $LaGaO_3$-based oxide. In the present study, therefore, effects of Fe doping on the oxide ion conductivity in LSGM were studied systematically. In addition, the power generating characteristics of fuel cells using Fe-doped LSGM were further studied.

Experimental

Sample preparation.—Calculated amounts of commercial La_2O_3 (Wako, 99.99% purity), $SrCO_3$, MgO (Wako, 99.9% purity), Ga_2O_3 (Kishida, 99.99% purity), and Fe_2O_3 (Kishida, 99.5%) were mixed in a Al_2O_3 mortar with a pestle and then precalcined at 1273 K for 6 h. Since the highest oxide ion conductivity was attained at $La_{0.8}Sr_{0.2}Ga_{0.8}Mg_{0.2}O_3$, the effects of Fe doping on oxide ion conductivity were studied at this composition. In order to clarify the effects of the Fe dopant on the electrical conductivity, the total amount of dopant in the Ga site was fixed at 20 mol % throughout this study. The resulting powders were pulverized and isostatically pressed into a disk (20 mm in diameter and 0.6 mm in thickness) at 274.6 MPa in vacuum. The disks were finally sintered at 1773 K for 6 h. X-ray diffraction (XRD) measurement was performed to analyze the purity of the obtained disk by XRD meter (Rigaku Rint 2000) with Cu Kα line. It confirmed that the single phase of $LaGaO_3$ perovskite was always obtained in this study.

Characterization of the obtained sample.—The electrical conductivity was measured as a function of temperature and oxygen partial pressure by a conventional dc four-probe method with a gas flow system. Each measurement was performed for longer than 1 h at least at each temperature and oxygen partial pressure to confirm a stable conductivity. The partial pressure of oxygen was controlled by mixing N_2, CO, or H_2 with O_2, and the oxygen partial pressure was monitored by CaO-stabilized ZrO_2 oxygen sensor that was attached close to the sample in the measurement cell. The transport number of oxide ion was estimated by the electromotive force of the H_2-O_2

* Electrochemical Society Active Member.
z E-mail: isihara@cc.oita-u.ac.jp

S0013-4651(99)09-056-4 CCC: $7.00 © The Electrochemical Society, Inc.

gas concentration cell. The oxygen partial pressure of the fuel gas was adjusted by adding 3 vol % H_2O to H_2.

In order to estimating the valence number of Fe in $LaGaO_3$-based oxide, electron spin resonance (ESR) measurements were performed with Broker EPR 380. The sample was calcined in H_2, He, and O_2 atmosphere at 1173 K for 3 h. Before measuring, the sample was evacuated at room temperature.

Application for electrolyte of solid oxide fuel cell.—In this study, a single-planer-type fuel cell was always fabricated by using the Fe-doped $LaGaO_3$ based oxide electrolyte for the power generating measurement. The obtained electrolyte disks were ground and polished with diamond wheels to 0.5 mm in thickness, and the specimen at this thickness was always used for SOFC application. In our previous study, it was found that $Sm_{0.5}Sr_{0.5}CoO_3$ exhibits a small overpotential at intermediate temperatures. Therefore, this $SmCoO_3$ based oxide was always used as the cathode of SOFC. Calculated amounts of Sm_2O_3 (Wako, 99.99% purity), $Sr(CH_3COO)_2$, and $Co(NO_3)_2$ were dissolved in a deionized water and heated to dryness with stirring. The obtained precursors were calcined at 1473 K for 6 h in air. Formation of single-phase $SmCoO_3$ perovskite oxide was confirmed by XRD analysis. The commercial NiO (Wako, 99.9%) without further purification was always used as the precursor of the anode. Slurries of the obtained cathode oxide and NiO were prepared by using *n*-butyl acetic acid as a solvent. About 30 mg of the slurry consisting of NiO- or Sr-doped $SmCoO_3$ were applied on one face of $LaGaO_3$ disks (5 mm in diam) by painting with a brush, respectively, followed by calcining at 1173 K for 10 min. Before measurement of power generating characteristics, NiO was reduced to Ni in a hydrogen stream at 1273 K.

The electrical power generating characteristics of a single SOFC were measured with the four-probe method using humidified hydrogen (3 vol % H_2O) as a fuel and oxygen as an oxidizing agent. The current density was controlled with a galvanostat (Hokuto HA301). It is also noted that the theoretical electromotive force estimated by the Nernst equation is 1.10 V at 1273 K under the condition used. Each gas was fed at 100 mL min^{-1}, and molten Pyrex glass was used for sealing the cells. The overpotential of the electrode was measured with a current interrupting method. A current pulse generated with the current pulse generator (Hokuto Denko, HC-111) was applied across the cathode and the anode, and the transient potential across the test electrode and the reference electrode, which was put at the side of the cathode, was analyzed with a digital spectrum analyzer (Takeda Riken TR-9404).

Results and Discussion

Valence number of Fe in the crystal lattice of $LaGaO_3$.—Figure 1 shows the XRD patterns of Fe-doped $LaGaO_3$ based oxide. These patterns mainly consist of peaks from the $LaGaO_3$ perovskite phase. Therefore, the main phase of the specimens was $LaGaO_3$ perovskite, however, some weak peaks which can be assigned to $LaSrGaO_4$ were observed on the XRD pattern of $LaGaO_3$-based oxide doped with more than 5 mol % of Fe. However, no diffraction peak from an oxide containing Fe was observed. Consequently, it can be said that the substitution of Ga with Fe in $LaGaO_3$-based oxide was performed at Fe contents smaller than 7 mol %.

In order to clarify the change in the defect concentration, determining the valence number of Fe in the lattice is of great importance. In this study, the valence number of oxide ion was measured with ESR. Figure 2 shows the ESR spectra of $La_{0.8}Sr_{0.2}Ga_{0.2}Mg_{0.19}Fe_{0.01}O_3$ after calcination in H_2, He, and O_2 atmosphere. It is reported that trivalent Fe is very sensitive to ESR measurement.[14] After calcining in H_2, the color of the specimens changed from dark brown to light azure. It is clearly shown in Fig. 2 that ESR signals were observed at *g* values of 4.20 and 2.40 after calcining in H_2. This signal is the typical one for an octahedral Fe(III). Therefore, it is suggested that iron substituted at the Ga site in the perovskite lattice and the valence number of most of the doped Fe is trivalent. Considering the stable valence and the coordination number, this is reasonable. On the other hand, the intensity of the ESR signal at a *g* value of 4.12 decreased, and a new broadening ESR signal appeared by calcination in O_2 at 1173 K, as shown in Fig. 2. It is also noted that the color of the specimens returned to the original color of dark brown. Since the intensity of the ESR signal assigned to Fe(III) was further weakened by calcination in an atmosphere at higher p_{O_2}, it seems likely that some part of Fe(III) was oxidized to Fe(IV), albeit a very limited amount. Although the number of the iron compounds consisting of Fe(IV) is very limited, it was reported that Fe(IV) is formed in perovskite-type oxide.[15] However, considering the stable valence number and strong ESR signal at $g = 4.20$, trivalent iron is dominant species both in O_2 and H_2 atmosphere. It is also noted that the ionic radius of Fe^{3+} is 64 pm, which is almost the same as that of Ga^{3+}, 62 pm.

Effects of Fe dopant in Ga site on oxide ion conductivity.—Figure 3 shows the electrical conductivity at 1223 K, and $p_{O_2} = 10^{-5}$ atm and the apparent activation energy for the electrical conductivity of Fe-doped LSGM as a function of Fe content. It is evident that the

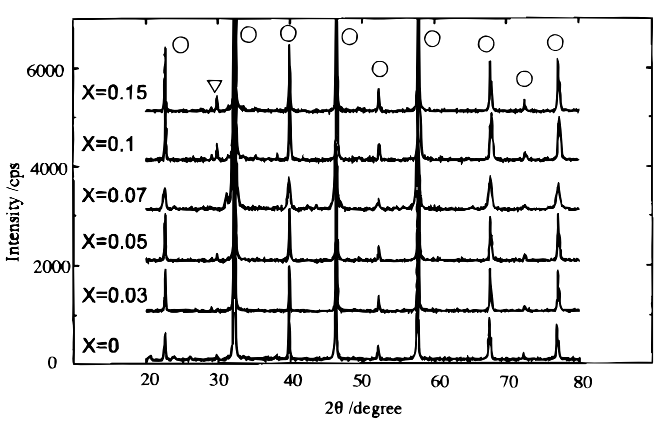

Figure 1. X-ray diffraction patterns of Fe doped $LaGaO_3$ based oxide. (○) $LaGaO_3$, (▽) $SrLaGaO_4$.

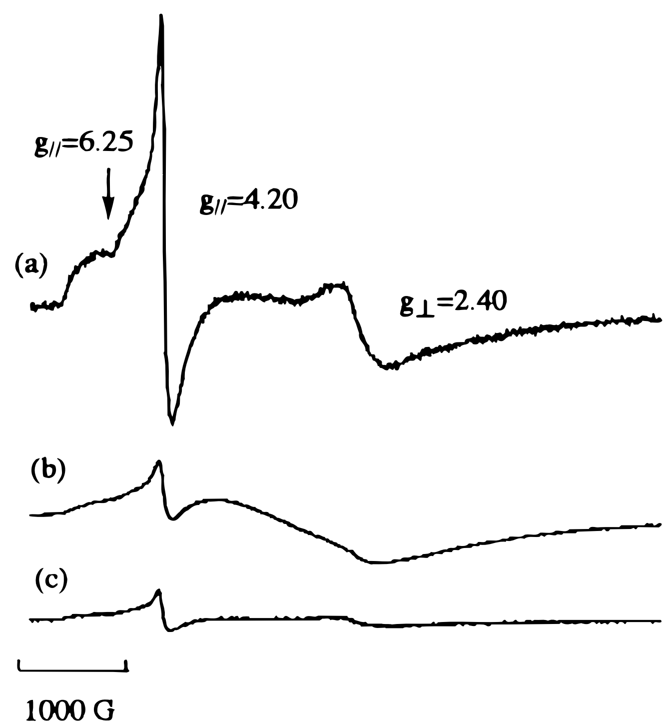

Figure 2. ESR spectra of $La_{0.8}Sr_{0.2}Ga_{0.8}Mg_{0.19}Fe_{0.01}O_3$ after calcination in (a) H_2, (b) He, and (c) O_2 at 1123 K for 3 h.

S0013-4651(99)09-056-4 CCC: $7.00 © The Electrochemical Society, Inc.

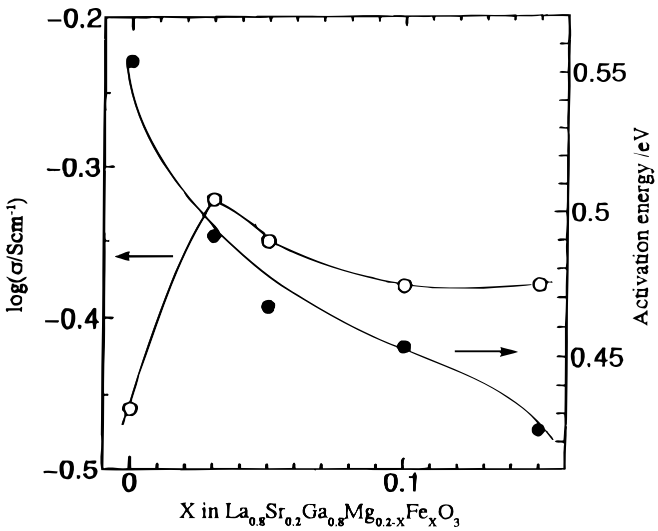

Figure 3. Electrical conductivity at 1223 K, $p_{O2} = 10^{-5}$ atm and apparent activation energy for conductivity in $La_{0.8}Sr_{0.2}Ga_{0.8}Mg_{0.2-x}Fe_xO_3$ as a function of x value. (○) Conductivity, (●) activation energy.

electrical conductivity increased with increasing Fe content, attaining a maximum value at $x = 0.03$ in $La_{0.8}Mg_{0.2}Ga_{0.8}Ga_{0.2-x}Fe_xO_3$. Although the formation of a secondary phase cannot be observed in the XRD pattern as shown in Fig.1, the electrical conductivity gradually decreased with increasing Fe content in the range of x values higher than 0.05. This may result from a limit in solid solution of Fe in the Ga site of $LaGaO_3$. In any case, it is obvious that the highest conductivity was attained at $x = 0.03$ ($La_{0.8}Mg_{0.2}Ga_{0.8}Ga_{0.17}Fe_{0.03}O_3$ denoted as LSGMF).

Figure 4 shows the electrical conductivity as a function of oxygen partial pressure. Since the electrical conductivity decreases with decreasing oxygen partial pressure, it is clear that the electronic hole conduction is present in high oxygen partial pressure by doping Fe and becomes significant when the amount of Fe is higher than 10 mol %. The order of p_{O2} dependence of conductivity is estimated to be *ca.* 0.025 when 15 mol % Fe was doped for the Ga site. Therefore, oxide ion conductivity is still dominant at this composition. To explain hole conduction at high oxygen partial pressure, the following equations can be incorporated into a mass-balance

$$\frac{3}{2}O_2 = 2V_M''' + 6h^{\bullet} + 3\ O_o^{\times} \quad [1]$$

$$2V_M''' + 3VO^{\bullet\bullet} = i \quad [2]$$

Here, M=Ga or La and i means an electrically neutral lattice point. These equations show that three molecules of the excess oxygen are incorporated into the lattice by the formation of Fe^{4+}, and the oxygen vacancy disappears by the introduction of excess oxygen. According to this equation, the hole concentration should increase with $p_{O2}^{3/16}$ and the hole conductivity also increase with the same p_{O2} dependence. On the other hand, the amount of the oxygen vacancy decreases, resulting in decreased oxide ion conductivity. The total conductivity is the sum of the hole and oxide ion conductivity, with the oxide ion conductivity being dominant in these Fe-doped $LaGaO_3$-based oxides. Therefore, it is considered that the p_{O2} dependence of the conductivity at high oxygen partial pressure becomes much smaller than 3/16. On the other hand, the electrical conductivity was almost independent of the oxygen partial pressure from $p_{O2} = 10^{-5}$ to 10^{-21} atm at such a high Fe doping amount. This suggests that the oxide ion conductivity is also stable in samples doped with Fe at more than 10 mol % in Ga sites. This is explained by the stability of Fe^{3+} over a wide range of oxygen partial pressure. On the other hand, electronic hole conduction was hardly observed at Fe content less than 5 mol %. Therefore, it is expected that the oxide ion conductivity was stably exhibited on the specimens for which the amount of doped Fe was less than 5 mol %. Since the electrical conductivity increased by doping Fe in this range, doping Fe to the Ga site seems to be effective for increasing the oxide ion conductivity. It is also noted that no electronic conduction behavior was observed on all specimens. Consequently, doping Fe to $LaGaO_3$-based oxide yields electronic hole conduction (p-type semiconduction), but no electronic conduction (n-type semiconduction).

Figure 5 shows the temperature dependence of the transport number of oxide ion, estimated with the H_2-O_2 gas concentration cell. It is clear that the high transport number of oxide ion is exhibited on all specimens. This is in good agreement with the result of p_{O2} dependence of the electrical conductivity in Fig. 4. The estimated transport number of oxide ion decreased with decreasing temperature,

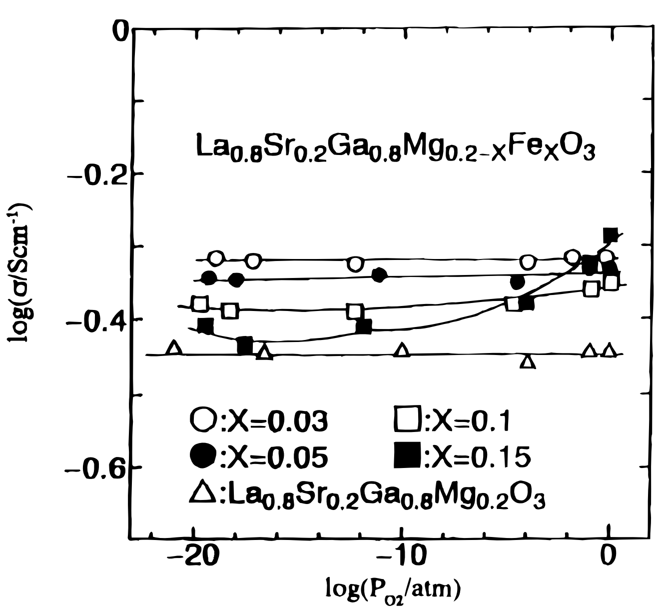

Figure 4. Electrical conductivity of LSGMF at 1123 K as a function of oxygen partial pressure.

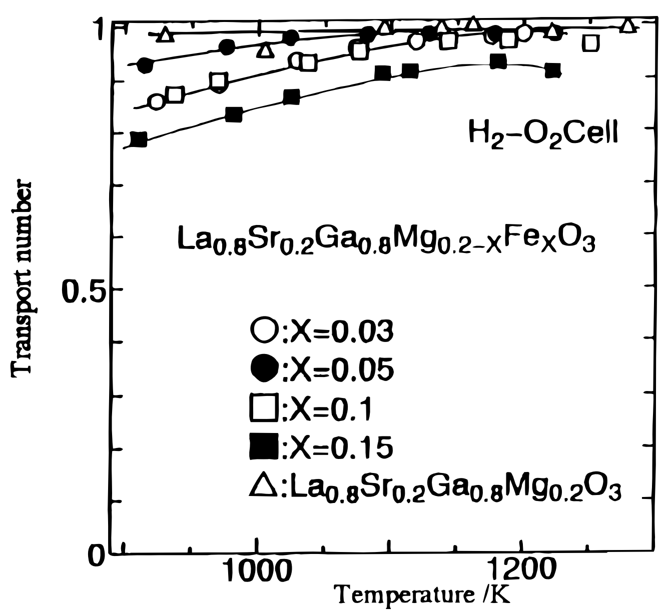

Figure 5. Temperature dependence of the transport number of oxide ion in LSGMF. Transport number was estimated with the electromotive force in H_2-O_2 cell.

S0013-4651(99)09-056-4 CCC: $7.00 © The Electrochemical Society, Inc.

since hole conduction became significant with decreasing temperature. It was reported that the excess oxygen is increased by decreasing temperature for the $LaCoO_3$- or $LaMnO_3$-based oxides.[16,17] Considering Eq. 1 and 2, the increase in the excess oxygen causes a decrease in the oxide ion conductivity due to the reduced amount of oxygen vacancies. However, all specimens exhibited a transport number higher than 0.8 at all temperatures examined. Compared to Co-doped $LaGaO_3$-based oxide, the Fe-doped oxide exhibited a higher transport number at all compositions. This may result from the stable valence number of Fe^{3+} in $LaGaO_3$ lattice.

Figure 6 shows the comparison of the oxide ion conductivity of LSGM doped with Co and Fe. It is clear that both LSGMF and LSGMC exhibits a higher oxide ion conductivity than LSGM. Doping Co decreased the activation energy for electrical conduction, however, activation energy of LSGMF is almost the same as that of LSGM. As a result, LSGMF exhibited a slightly higher oxide ion conductivity than that of LSGMC at high temperature. However, at low temperature, LSGMC exhibits the higher conductivity. On the other hand, hole conduction was significant in LSGMC, but not so significant for LSGMF. In case of LSGMC in our previous study, the valence number of Co was divalent. Therefore, a higher transport number of LSGMF than that of LSGMC could be explained by the higher stability of Fe^{3+} than that of Co^{2+}. Considering the higher transport number of oxide ion, LSGMF is also attractive as a solid electrolyte for SOFC. On the other hand, the amount of the oxygen vacancy was decreased by doping Fe^{3+} instead of Mg^{2+}. In spite of the decreased amount of oxygen vacancy, the improved oxide ion conductivity seems to be explained by the improved mobility of oxide ion. This is because the ionic size of Fe^{3+} (64 pm) is intermediate between Ga^{3+} (62 pm) than Mg^{2+} (66 pm). Consequently, the origin of the dopant effect of Fe seems to be the release of the local stress in the lattice due to the mismatch in ionic size. It is also noted that the optimized amount for Fe doping is at the small level of 3 mol %, because an excess of Fe decreased the amount of oxygen vacancy.

Power generation characteristics of SOFC using LSGMF as electrolyte.—For the application of LSGM as electrolyte of SOFC, it was found that $Sm_{0.5}Sr_{0.5}CoO_3$ and Ni were appropriate for the cathode and the anode, respectively.[3] By using the same cathode and anode, the power generating characteristics were studied with Fe-doped LSGM used for the electrolyte in this study. Figure 7 shows the maximum power density of the cell using Fe-doped LSGM at 1073 K as a function of the Fe amount. In this figure, the conductivity of LSGMF at 1123 K was also shown. It is obvious that the maximum power density was increased with increasing amount of Fe and attained to the maximum value of 700 mW/cm^2 at $x = 0.03$. In addition, the open-circuit potential of this cell attained a value of 1.09 V, which almost corresponds to the theoretical value of 1.10 V. At this composition, it is clear that the electrical conductivity also attains a maximum value. Therefore, it is anticipated that the improved power density by doping Fe was obtained by increasing the oxide ion conductivity.

The internal resistance of the cell using LSGMF as the electrolyte was estimated with the current interruption method and the estimated ohmic loss (IR loss), overpotential of the cathode (η_{CA}), and the anode (η_{AN}) are shown in Fig. 8 against the amount of Fe content in the electrolyte. It is clear that the main internal resistance of the present cell was the ohmic loss which almost corresponded with the value estimated from the conductivity of the electrolyte. The cathodic or the anodic overpotential are generally believed to be independent of the electrolyte conductivity; however, both overpotentials were decreased by a decrease in the Fe content and attained minimum values at $x = 0.03$. This tendency is more apparent on the anodic overpotential. Consequently, the improved power density was not simply brought about by the decrease in the electrical resistance of the electrolyte but also by the decrease in the overpotential of the electrodes, in particular the anode.

The temperature dependence of the maximum power density together with the open-circuit potential of LSGMF cell is shown in Fig. 9. The open-circuit potentials were slightly smaller than the theoretical value when LSGMC is used as the electrolyte; however, LSGM and LSGMF cells exhibited open-circuit potentials close to the theoretical potential of 1.1 V at all temperatures. This is also in good agreement with the results of the oxide ion transport-number measurement. On the other hand, a notably large power density was sustained at low temperature (higher than 100 mW/cm^2 at 873 K) on the LSGMF cells given the fact that the thickness of the electrolytes was 0.5 mm. The power density of the LSGMF cell was smaller than that of the LSGMC cell at the examined temperatures range due to a slightly larger ohmic loss. However, the open-circuit potential of the LSGMF cell is higher than that of LSGMC cell and close to the theoretical value at all temperatures. Therefore, it is expected that the amount of electrochemically leaked oxygen was negligible in the LSGMF cell. Consequently, it is expected that the energy conversion efficiency in the LSGMF cell is higher than that of the LSGMC cell.

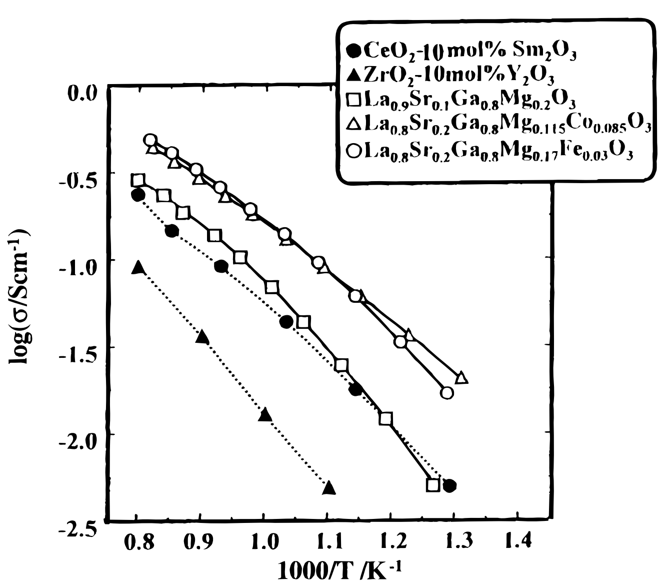

Figure 6. Comparison of the oxide ion conductivity of LSGM doped with Co and Fe with the conventional fluorite oxide.

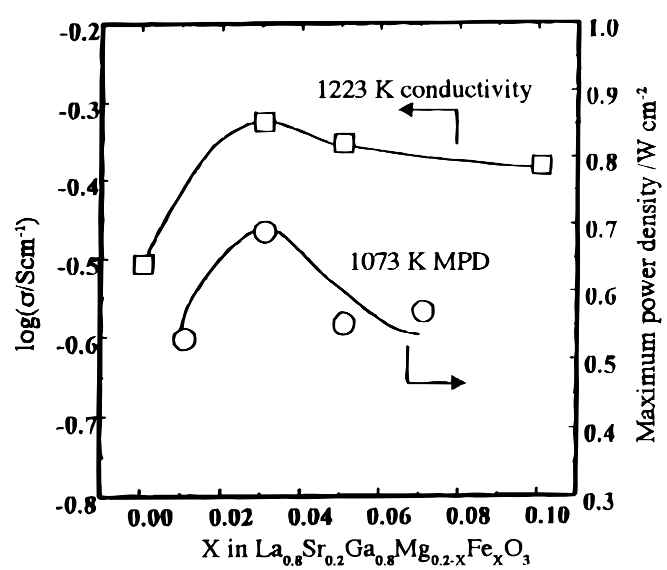

Figure 7. Maximum power density of the LSGMF fuel cell at 1073 K and oxide ion conductivity at 1123 K as a function of Fe content in electrolytes. Thickness of electrolyte; 0.5 mm. Cell: H_2 + 3 vol % H_2O, Ni$|La_{0.8}Sr_{0.2}Ga_{0.8}Mg_{0.2-x}Fe_xO_3|Sm_{0.5}Sr_{0.5}CoO_3$, O_2. (○) Maximum power density, (□) conductivity.

S0013-4651(99)09-056-4 CCC: $7.00 © The Electrochemical Society, Inc.

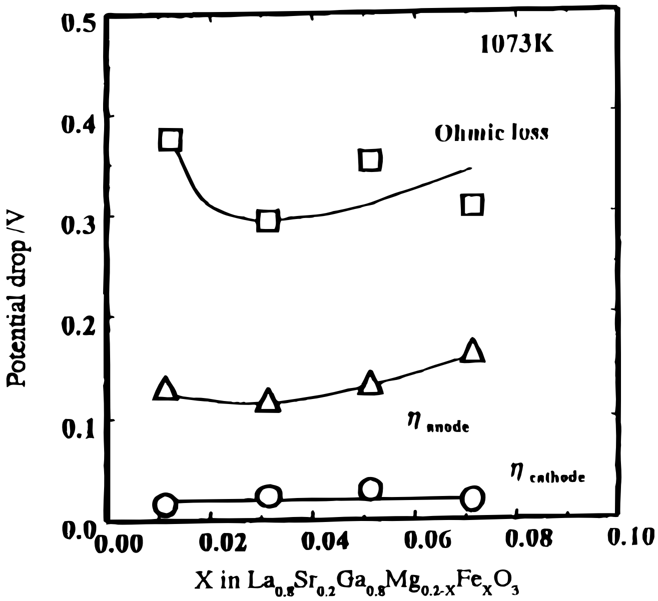

Figure 8. Ohmic loss, overpotential of anode, and cathode of the LSGMF cell at 1073 K as a function of Fe content in electrolytes. Anode, Ni; cathode, $Sm_{0.5}Sr_{0.5}CoO_3$, reference, Pt.

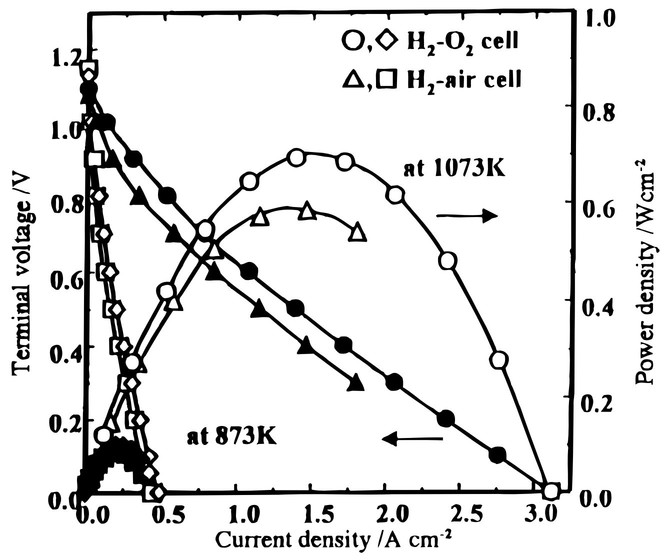

Figure 10. Effects of oxidant on the power generation characteristics of the LSGMF cell. Anode; Ni, Cathode; $Sm_{0.5}Sr_{0.5}CoO_3$; thickness of electrolyte, 0.5 mm.

From the efficiency point of view, LSGMF is a more attractive electrolyte than LSGMC.

In a commercial fuel cell, air is generally considered to be used for an oxidant. Therefore, in this work, the power generation characteristics of the LSGMF cell using air as the oxidant were studied. Figure 10 shows the comparison of the power generation characteristics of H_2-O_2 and H_2-air cells. It is considered that the open-circuit potential as well as the maximum power density decrease by decreasing the oxygen partial pressure. Although the open-circuit potential was not significantly changed, the use of air for the oxidant resulted in a decrease in the maximum power density at 1073 K. However, that reduction in the power density was not significant. The same tendency was also observed for the LSGMC cell. It is anticipated that the decrease in the oxygen partial pressure will decrease the adsorption rate of oxygen on the cathode and, consequently, the power density will be decreased due to the increased cathodic overpotential. However, the same decrease in the power density was hardly observed at 873 K. It seems that the rate-limiting step for the cathodic reaction was changed from the adsorption controlled process to the diffusion controlled process with decreasing temperature. Therefore, the increase in the cathodic overpotential does not seem to be significant in spite of the decrease in the oxygen partial pressure at intermediate temperatures. Consequently, the decrease in the power density by changing the oxidant from O_2 to air was not significant at intermediate temperatures.

Figure 11 shows the impedance of the anode and cathode of the LSGMF cell at the open-circuit condition. It is clear that the anodic overpotential was far larger than the cathodic one. Therefore, in the present cell, it is considered that the anodic reaction is the rate-determining step and $Sm_{0.5}Sr_{0.5}CoO_3$ is highly active to the cathodic reaction, namely, the dissociation of oxygen molecules into oxide ions at low temperature. The similar impedance plots for H_2-air cell were also measured, and the results are superimposed in Fig. 11. Compared with the impedance plots of the H_2-O_2 cell, the semicircle for the anodic reaction was hardly changed; however, obviously, that for the cathodic reaction was increased on the H_2-air cell. In particular, the semicircle at low frequencies was increased by changing the oxidant from O_2 to air. It is clear that the semicircle of the cathodic overpotential is slightly depressed. This suggests that the cath-

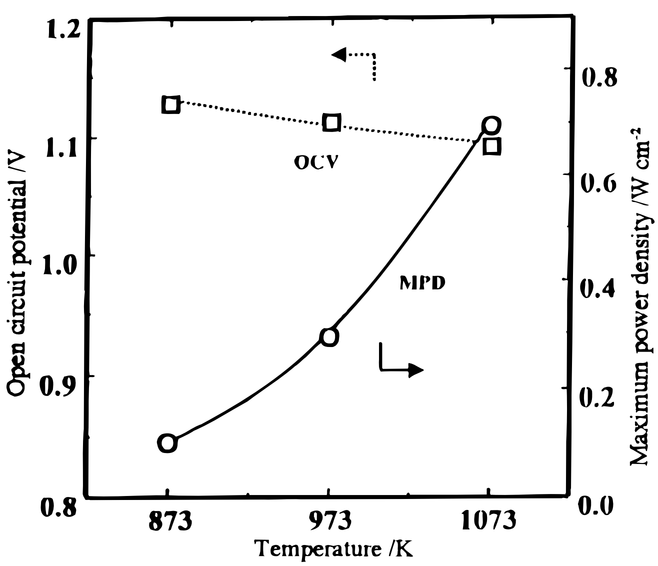

Figure 9. Temperature dependence of the maximum power density and open-circuit potential of LSGMF cell.

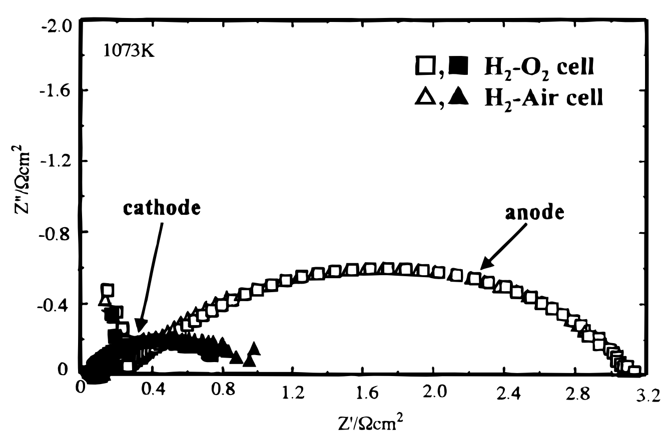

Figure 11. Complex impedance plane plots of anode and cathode of the LSGMF cell at the open-circuit condition at 1073 K. Cell: H_2 + 3 vol % H_2O, Ni|$La_{0.8}Sr_{0.2}Ga_{0.8}Mg_{0.2-x}Fe_xO_3$|$Sm_{0.5}Sr_{0.5}CoO_3$, O_2, or air.

S0013-4651(99)09-056-4 CCC: $7.00 © The Electrochemical Society, Inc.

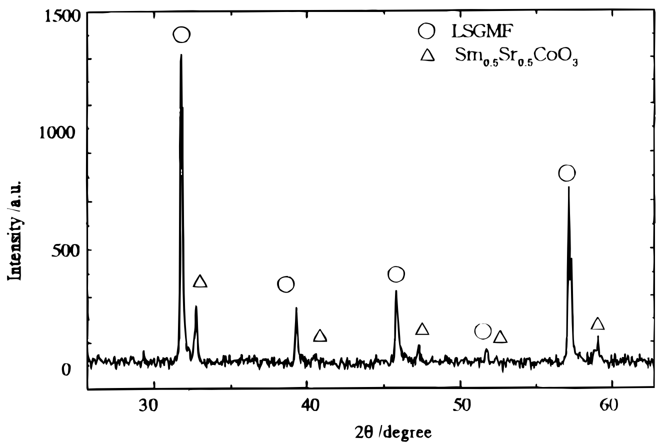

Figure 12. XRD pattern of the LSGMF cell at the cathode side after measurement of the power generating characteristic at 1273 K.

odic reaction consists of at least two steps. It is anticipated that the cathodic reaction mainly consists of the adsorption and the following diffusion process. It is generally expected that semicircle assigned to the diffusion step appears in a lower frequency region. Decreasing the oxygen partial pressure will decrease the surface oxygen concentration. Consequently, it seems likely that the diffusion resistance in the cathodic reaction is increased by changing the oxidant from O_2 to air due to the increase in the oxygen concentration difference between the cathode and the electrolyte surface. Anyway, it is obvious that the decrease in power density by changing from O_2 to air as an oxidant is caused by the enlarged cathodic overpotential.

It was reported that Co-based perovskite cathode oxide was easily reacted with YSZ to form a secondary phase. Therefore, the reactivity of $SmCoO_3$-based cathode with LSGMF was examined with XRD measurement before and after the power measurement. Figure 12 shows the XRD pattern of LSGMC cell at the cathode side after the measurement of the power characteristics. Clearly, only the diffraction peaks from LSGMF and $SmCoO_3$ were observed, and there were no observable diffraction peaks from the secondary phase nor changes in diffraction angle in Fig. 12. Consequently, the reactivity of LSGMF to $SmCoO_3$-based oxide cathode was sufficiently low for the application of SOFC. On the other hand, durability of the power density of the LSGMF cell was also measured, and it was confirmed that the decrease in the power density was insignificant within the initial few 100 h. Therefore, it can be said that substitution of the part of Mg in Ga site of $LaGaO_3$ with Fe is effective in improving the oxide ion conductivity and Fe-doped LSGM is the attractive electrolyte for an intermediate temperature SOFC.

Conclusion

It is generally believed that doping a transition metal cation is undesirable for oxide ion conductivity, since electronic conduction emerges. However, this study revealed that doping 3 mol % Fe to the Ga site of LSGM is effective for increasing the oxide ion conductivity. Although an excess amount of Fe results in significant hole conduction at high oxygen partial pressures, the oxide ion conductivity in $La_{0.8}Sr_{0.2}Ga_{0.8}Mg_{0.17}Fe_{0.03}O_3$ was stably exhibited in the p_{O2} range from 1 to 10^{-21} atm.

Although the power density was slightly smaller than that of the cell using Co-doped LSGM for the electrolyte, almost the theoretical open-circuit potential was exhibited on the cell using the Fe-doped LSGM. Therefore, it can be said that the usage of LSGMF for the electrolyte is also promising for decreasing the operating temperature of SOFC. The maximum power density of the cell was slightly decreased by changing the oxidant from O_2 to air; the cell using air as the oxidant still exhibited a power density of 600 mW/cm^2 at 1073 K in spite of the usage of 0.5 mm thickness of electrolyte. Although it was reported that Ga was volatilized from LSGM in reducing atmosphere by Yamaji *et al.*,[18] no significant change in composition was observed after operation at 1073 K for 200 h by the elemental analysis with the inductively coupled plasma emission spectroscopy (ICP). In addition, no significant decrease in power density as well as open-circuit potential were observed over 200 h at 1073 K. Since oxygen is always supplied through the electrolyte, it seems that Ga volatilization hardly occurred under SOFC operation condition, and it seems to cause no serious problem for SOFC application. Consequently, the authors believe that SOFC operating at temperature lower than 1073 K can be successfully developed by using Co- or Fe-doped LSGM as the electrolyte of SOFC.

Acknowledgment

Part of this study was supported by Nissan research grant. Part of this study was supported by a Grant-in-Aid from the Ministry of Education, Science, Sports and Culture of Japan.

Oita University assisted in meeting the publication costs of this article.

References

1. N. Q. Minh and T. Takahashi, *Science and Technology of Ceramic Fuel Cells*, Elsevier, Amsterdam (1995).
2. B. C. H. Steele, *J. Power Sources,* **49,** 1 (1994).
3. M. Godickemeier, K. Sasaki, L. I. Gauckler, and I. Riess, *J. Electrochem. Soc.,* **144,** 1635 (1997).
4. I. Yasuda and M. Hishinuma, Abstract 2141, p. 2504, The Electrochemical Society and International Society of Electrochemistry Meeting Abstracts, Vol. 97-2, Paris, France, Aug 31-Sept 5, 1997.
5. A. Atkinson, *Solid State Ionics,* **95,** 249 (1997).
6. S. de Souza, S. J. Visco, and L. C. de Jonghe, *J. Electrochem. Soc.,* **144,** L35 (1997).
7. T. Ishihara, H. Matsuda, and Y. Takita, *J. Am. Chem. Soc.,* **116,** 3801 (1994).
8. T. Ishihara, H. Matsuda, and Y. Takita, *Solid State Ionics,* **79,** 147 (1995).
9. M. Feng and J. B. Goodenough, *Eur. J. Solid State Inorg. Chem.* **31,** 663 (1994).
10. P. N. Huang and A. Petric, *J. Electrochem. Soc.,* **143,** 1644 (1996).
11. J. W. Stevenson, T. R. Armstrong, D. E. McCready, L. R. Pederson, and W. J. Weber, *J. Electrochem. Soc.,* **144,** 3613 (1997).
12. R. T. Baker, B. Gharbage, and F. M. B. Marques, *J. Electrochem. Soc.,* **144,** 3130 (1997).
13. T. Ishihara, H. Furutani, M. Honda, T. Yamada, T. Shibayama, T. Akbay, N. Sakai, H. Yokokawa, and Y. Takita, *Chem. Mater.,* **11,** 2081 (1999).
14. S. Bordiga, R. Buzzoni, F. Geobaldo, C. Lamberti, E. Giamello, A. Zecchina, G. Leofanti, G. Petrini, G. Tozzola, and G. Vlaic, *J. Catal.,* **158,** 486 (1996).
15. T. C. Gibb, *J. Chem. Soc., Dalton Trans.,* 1447 (1986).
16. J. Mizusaki, J. Tabuchi, T. Matsuura, S. Yamauchi, and K. Fueki, *J. Electrochem. Soc.,* **136,** 2082 (1989).
17. J. Mizusaki, *Solid State Ionics,* **52,** 79 (1992).
18. K. Yamaji, T. Horita, M. Ishikawa, N. Sakai, and H. Yokokawa, *Solid State Ionics,* **108,** 415 (1998).